*Bull. Mater. Sci.* (2022) 45:29
https://doi.org/10.1007/s12034-021-02605-0


# Low-temperature sintering processes of $Mg_{0.8}Zn_{0.2}TiO_3$ through $K_{0.5}Na_{0.5}VO_3$ and $Bi_2O_3$ addition correlated to the dielectric properties

**S R A RANI[1,2], A P SAMBAYU[1] and S SUASMORO[1,*]**
[1]Department of Physics, Institut Teknologi Sepuluh Nopember, Kampus ITS Sukolilo, Surabaya 60111, Indonesia
[2]Department of Physics, Universitas Islam Negeri Alauddin, Jl. Sultan Alauddin, Makassar 90221, Indonesia
*Author for correspondence (suasm@its.ac.id)

MS received 5 July 2021; accepted 30 September 2021

**Abstract.** This study reports the sintering of $Mg_{0.8}Zn_{0.2}TiO_3$ (MZT) with an addition of $K_{0.5}Na_{0.5}VO_3$ (KNV) and $Bi_2O_3$. The sintering temperature was performed at 950°C for 4 h and attained a maximum relative density of 97.71% in a composition of 85% mol MZT–10% mol KNV–5% $Bi_2O_3$ (MZT85). Structure, microstructure and phase present in the sample were analysed using X-ray diffraction, scanning electron microscopy and energy-dispersive X-ray spectroscopy. $MgZnTiO_3$, $KNaVO_3$ and $BiVO_4$ were found, besides, the non-crystalline phase was also detected and supposed to be the $Bi_2O_3$ melted amorphous phase. Furthermore, with an increase of the lattice parameter and cell volume of samples, it was believed that the sintering aid dissolved partially in the MZT matrix. The electrical properties characterization discovered that at low frequencies (1 Hz–32 MHz) a broader range of space charge polarization was observed, meanwhile, at high frequency (X-band) an enhancement of the permittivity and quality factor Qxf. The relative permittivity $\varepsilon_r \approx 16.08$, the dielectric loss (tan $\delta$) $\sim 10^{-2}$ and Qxf = 11.386 GHz at 10 GHz for the MZT85 sample was observed.

**Keywords.** $Mg_{0.8}Zn_{0.2}TiO_3$; dielectric; solid-state reaction; sintering.

## 1. Introduction

$MgTiO_3$-based materials are known as one of the materials for a high-frequency application, such as resonators, microwave oscillators and wireless technologies. These materials exhibit a moderate dielectric constant, low dielectric loss (i.e., a high-quality factor), and have good temperature stability [1–6]. This motivated researchers to investigate $MgTiO_3$-based ceramics involving methods of fabrication to improve performance, otherwise make it low-cost and easier fabrication processes including varying powder preparation techniques [7,8]. It was reported that $MgTiO_3$-based ceramics exhibited good microwave dielectric properties ($\varepsilon_r \sim 15$) and good quality factor (Qxf) $\sim 1$ to $3 \times 10^4$ at frequency 7.7 GHz [7]. However, the weakness of the dielectric $MgTiO_3$ needs a very high sintering temperature to get a reasonable density at approximately 1400°C.

The high sintering temperature processes increased manufacturing cost and difficulty to accomplish a suitable electrode. Considering to utilize Ag as an electrode material (melting point ≈962°C) [9], the sintering process is required at a lower than the melting point of Ag, e.g., ≈ 950°C. Many efforts were carried out to reduce the sintering temperature and to improve the performance of $MgTiO_3$ ceramics, such as performing dopant, additive, and varying the synthesis process [7,10–12]. Ermawati *et al* [7,10] synthesized Zn-doped $MgTiO_3$ through a dissolved method to promote density, improve the purity of the main phase, increase permittivity, and accelerate the reaction at 550°C. Pan *et al* [13] synthesized (1–*x*) $MgTiO_3$–*x*$Ca_{0.8}Sr_{0.2}TiO_3$ to make better dielectric properties, sintered at 1200–1325°C; however, it caused changes in the surface microstructure of the material, fast grain growth, and possessed maximum density (3.65–3.77 g $cm^{-3}$). Alternatively, Kathait *et al* [14] used a modification of the sintering cycle as was carried out on 0.02 K $(Ta_{0.5}Nb_{0.5})O_3$−0.98$BaTiO_3$ to modify their characteristics.

It was common that an alteration sintering through additive material was utilized to enhance the shrinkage mechanism as well as its characteristics [15]. An effort to reduce sintering temperature has been carried out by the addition of a lower melting point material. Saukani and Suasmoro [11] reported that through $Bi_2O_3$ addition in $Mg_{0.8}Zn_{0.2}TiO_3$ (MZT) the sintering temperature reduced to 1100°C and attained a density of 3.67 g $cm^{-3}$ [11]. Santhosh Kumar *et al* reported that the $V_2O_5$ additive successfully reduced the sintering temperature of $MgTiO_3$ up to 1100°C, which is due to the formation of the liquid phase [9]. Sebastian *et al* [16] reviewed that there are types of

Published online: 03 February 2022

co-fired ceramic material that are usually used in the sintering process at a temperature of $< 700°C$ called ultra-low-temperature co-fired ceramic and sintering process at a temperature of 700–1000°C so-called low-temperature co-fired ceramic. Some examples of materials as co-fired ceramics containing vanadate compositions include $Mg_3(VO4)_2$, $R_2V_2O_7$ (R = Ba, Sr, Ca, Mg and Zn), $NaCa_2Mg_2V_3O_{12}$, $LiZnVO_4$, $BaV_2O_6$, $Na_2BiMg_2V_3O_{12}$. Among the compositions of ceramic co-sintering agents includes vanadium and sodium, accordingly, and it can be considered that the composition of alkali–vanadium oxide can be used as a co-sintering agent. In the preliminary investigation, the alkali vanadate $K_{0.5}Na_{0.5}VO_3$ (KNV) was melted at temperatures ~530–550°C, furthermore, a sintered KNV at 525°C possessed a relative permittivity ~29.

Considering the similar types of structure ABO3, it can be expected that after KNV melts and proceeds to sinter, *viz.* accelerate shrinkage, then dissolves in the MZT matrix in the rest of the sintering process. The $Bi_2O_3$ will melt at 817°C then take place in the advancement of the final step of sintering. This study reported an effort pursuing reducing sintering temperature as low as 950°C, possessing good quality ceramics through addition of $K_{0.5}Na_{0.5}VO_3$ and $Bi_2O_3$ in $Mg_{0.8}Zn_{0.2}TiO_3$ (MZT) material in terms of densification, structure, microstructure and electrical properties, in which the last properties were compared with MZT sample.

## 2. Experimental

The composition of $(0.95–x)Mg_{0.8}Zn_{0.2}TiO_3–_xK_{0.5}Na_{0.5}VO_3–0.05Bi_2O_3$ ($x$ = 0.1–0.30) abbreviated as MZT(0.95–$x$) was prepared in two steps. First, the $Mg_{0.8}Zn_{0.2}TiO_3$ (MZT) and $K_{0.5}Na_{0.5}VO_3$ (KNV) compositions were prepared separately through the solid-state reaction of stoichiometric mixtures of raw materials, i.e., MgO, ZnO, $TiO_2$ for MZT, while $K_2CO_3$, $Na_2CO_3$, $V_2O_3$ for KNV, respectively. The raw materials were mixed in an attrition mill for 6 h and an angular velocity of 600 rpm in the ethyl alcohol environment, similar for both compositions. Afterwards, both slurries were dried and subjected to optimize calcination. Whereas, $Bi_2O_3$ was obtained by heating up $Bi(NO_3)_3$ powder at 730°C for 6 h. Second, mixed those three powders MZT, KNV and $Bi_2O_3$ in the desired composition using an attritor similar to the previous procedure, compacted into a pellet using a 13-mm die at a pressure of 100 MPa, and finally, pellets were sintered at 950°C for 4 h.

The density of sintered samples was measured employing Archimedes' principle. Structure and phase characterization were analysed using X-ray diffraction (XRD) data collected using Cu Kα radiation. Phase identification was carried out through Match2 software, while for the crystal structure analysis, the Rietveld refinement method was exploited. Scanning electron microscopy and energy-dispersive X-ray spectroscopy (SEM-EDX) was utilized for microstructure characterization on a thermally etched sample. Whereas the electrical properties evaluation was performed using two methods: impedance analyzer in the frequency range 1 Hz to $32 \times 10^6$ Hz and vector network analyzer in the frequency range $10^{9.9}$–$10^{10.1}$ Hz at room temperature.

## 3. Result and discussion

### 3.1 *Synthesis and sintering*

Figure 1a shows the XRD spectra of the main components for MZT(1–$x$) as a result of the first-step preparations. Previously, the MZT powder was subjected to synthesis at different temperatures and times to achieve almost single-phase. At moderate temperature 850°C, the MZT yield displays an important intensity. Therefore, a further test of

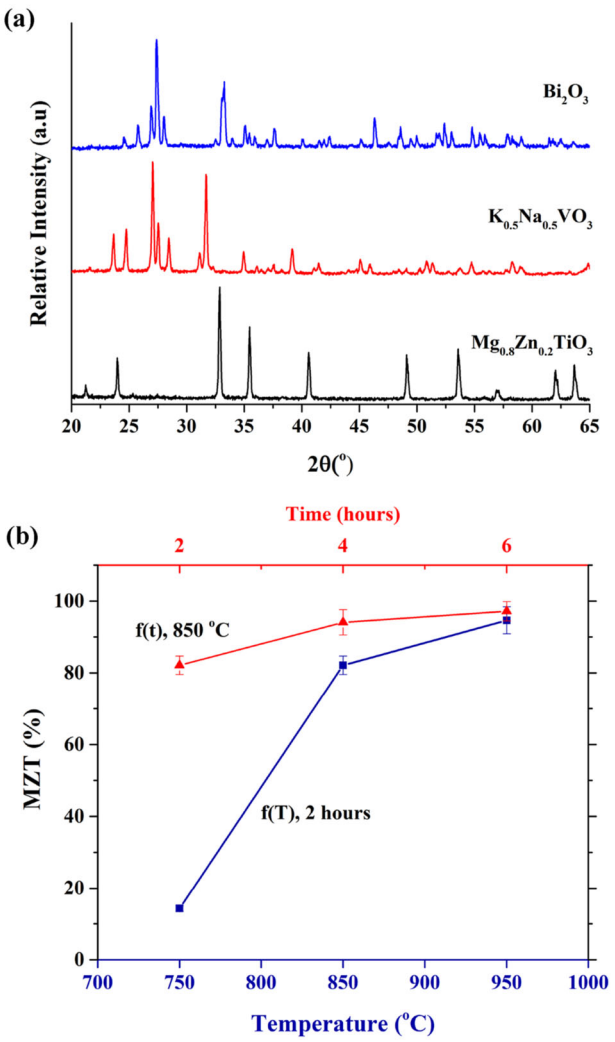


**Figure 1.** (**a**) X-ray diffraction pattern of $Mg_{0.8}Zn_{0.2}TiO_3$, $K_{0.5}Na_{0.5}VO_3$, $Bi_2O_3$ after optimum calcination processes. (**b**) The yield of $Mg_{0.8}Zn_{0.2}TiO_3$ after calcination at different temperatures for 2 h, and 850°C for different dwell times.

synthesis in different dwell times is then performed. Figure 1b presents the MZT yields evaluated based on XRD data and Rietveld's refinement. It shows that at 850°C for 4 h, the MZT reach more than 94%, and matched with crystallographic data rhombohedral—space group $R\bar{3}H$ for MZT [17]. This achievement is then considered as reasonable for an intermediate step of the synthesis.

Considering the phase diagram $V_2O_5$–$K_2O$ [18], when V/K = 1 the composition $KVO_3$ indicates a congruent melt at 514°C. The synthesis of KNV then takes place at < 514°C. Given that Na and K have similar alkali groups, a similar reason for the synthesis of $K_{0.5}Na_{0.5}VO_3$ from initial raw materials $V_2O_5$, $K_2CO_3$ and $Na_2CO_3$ was carried out at 500°C for 2 h. XRD examination of calcined powder poses a monoclinic crystal symmetry and space group *C2/c* having lattice parameters $a$ = 10.533 Å, $b$ = 9.977 Å and $c$ = 5.804 Å, while $\alpha = 90°$, $\beta = 104.17°$ and $\gamma = 90°$, respectively. Figure 1a shows the XRD patterns of the $Mg_{0.8}Zn_{0.2}TiO_3$, $K_{0.5}Na_{0.5}VO_3$, as well as $Bi_2O_3$.

The desired composition MZT(0.95–$x$) was performed simultaneously during the sintering processes. To achieve a good ceramic sintered at 950°C and moderate holding time of 4 h, the relative density should be taken as one indicator. Table 1 shows the density of sintered samples (0.95–$x$)MZT–0.05$Bi_2O_{3-x}$KNV. A relative density above 97.7% was achieved by MZT85 ($x$ = 0.10), which declined to 94% for MZT65 ($x$ = 0.30). These should be compared to MZT, which was sintered at 1400°C for 8 h to attain the relative density of 90% [7].

Further phase analysis was performed on the sintered sample, and figure 2 shows XRD patterns of those samples. The secondary phase was detected and identified as (Ka/Na)$VO_3$ and $Bi_4V_2O_{11}$ in the MZT65 sample, furthermore $Bi_2Ti_2O_7$ and $Bi_4V_2O_{11}$ detected in MZT75, while a small intensity identified as KNV present in MZT85. The deeper analysis of XRD data through Rietveld's refinement ensuing in lattice parameters are presented in table 1. It shows that a very small lattice parameter varies following the variation of MZT, though the cell volume is constant. In contrast, the cell volume is larger when it is compared to the initial calcined powder, besides the overall percentage of the MZT phase is higher than that of the initial percentage of the initial composition before sintering. It is then presumed that the sintering aid $Bi_2O_3$ and $K_{0.5}N_{0.5}VO_3$ are partly dissolved in the MZT matrix, and the rest performing secondary phase.

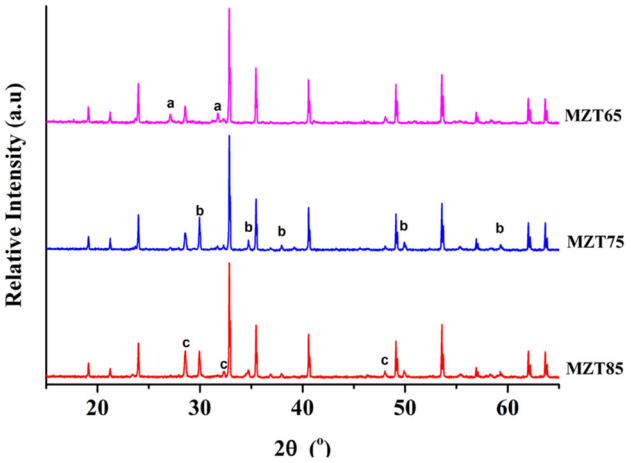


**Figure 2.** X-ray diffraction pattern after sintering of MZT$x$ samples (a = (Ka/Na)$VO_3$; b = $Bi_2Ti_2O_7$; c = $Bi_4V_2O_{11}$).

The microstructure analysis for samples is represented by MZT85 sample. Figure 3a shows a secondary electron mode image showing two population grains, spread regularly of the large grains, and colonies of small grains; furthermore,

**Table 1.** Lattice parameters of the phases present in the sintered sample analysed using Rietveld refinement of XRD data, the reliability factors are indicated.

| Sample | Phase identification | Relative density(%) | Mole percent (%) | Lattice parameter (Å) | | | Unit cell volume ($A^3$) | Reliability factor |
|---|---|---|---|---|---|---|---|---|
| | | | | *a* | *b* | *c* | | |
| MZT65 | (Mg/Zn)$TiO_3$ | 94.13 | 75.93(1) | 5.0603(3) | 5.0603(3) | 13.9112(9) | 308.5(0) | Rp = 10.2 |
| | (Ka/Na)$VO_3$ | | 20.36(1) | 10.5644(3) | 10.0531(9) | 5.8022(7) | 598.2(2) | Rwp = 13.4 |
| | $Bi_4V_2O_{11}$ | | 3.71(0) | 16.5959(3) | 5.5474(5) | 15.5344(4) | 1430.2(0) | Gof = 2,6 |
| MZT75 | (Mg/Zn)$TiO_3$ | 96.87 | 92.56(0) | 5.0604(1) | 5.0604(1) | 13.9119(4) | 308.5(0) | Rp = 9.9 |
| | $Bi_4V_2O_{11}$ | | 3.32(3) | 16.6062(1) | 5.5443(7) | 15.5467(7) | 1431.4(3) | Rwp = 13.2 |
| | $Bi_2Ti_2O_7$ | | 0.73(2) | 10.3271 (5) | 10.3271(5) | 10.3271(5) | 1101.4(1) | Gof = 2,7 |
| | (Ka/Na)$VO_3$ | | 3.39(3) | 10.6318(8) | 10.1402(5) | 5.7673(7) | 607.1(0) | |
| MZT85 | (Mg/Zn)$TiO_3$ | 97.71 | 92.38(1) | 5.0602(1) | 5.0601(1) | 13.9122(4) | 308.5(1) | Rp = 9.3 |
| | $Bi_4V_2O_{11}$ | | 6.93(1) | 16.5877 (0) | 5.5440(1) | 15.5702(3) | 1431.8(7) | Rwp = 13.9 |
| | $Bi_2Ti_2O_7$ | | 0.69(2) | 10.3321(7) | 10.3321(7) | 10.3321(7) | 1102.9(1) | Gof = 2.2 |
| MZT calcined | (Mg/Zn)$TiO_3$ | — | ≈100 | 5.0591(2) | 5.0591(2) | 13.9109(9) | 308.0(0) | Rp = 12.2<br>Rwp = 9.44<br>Gof = 1.28 |

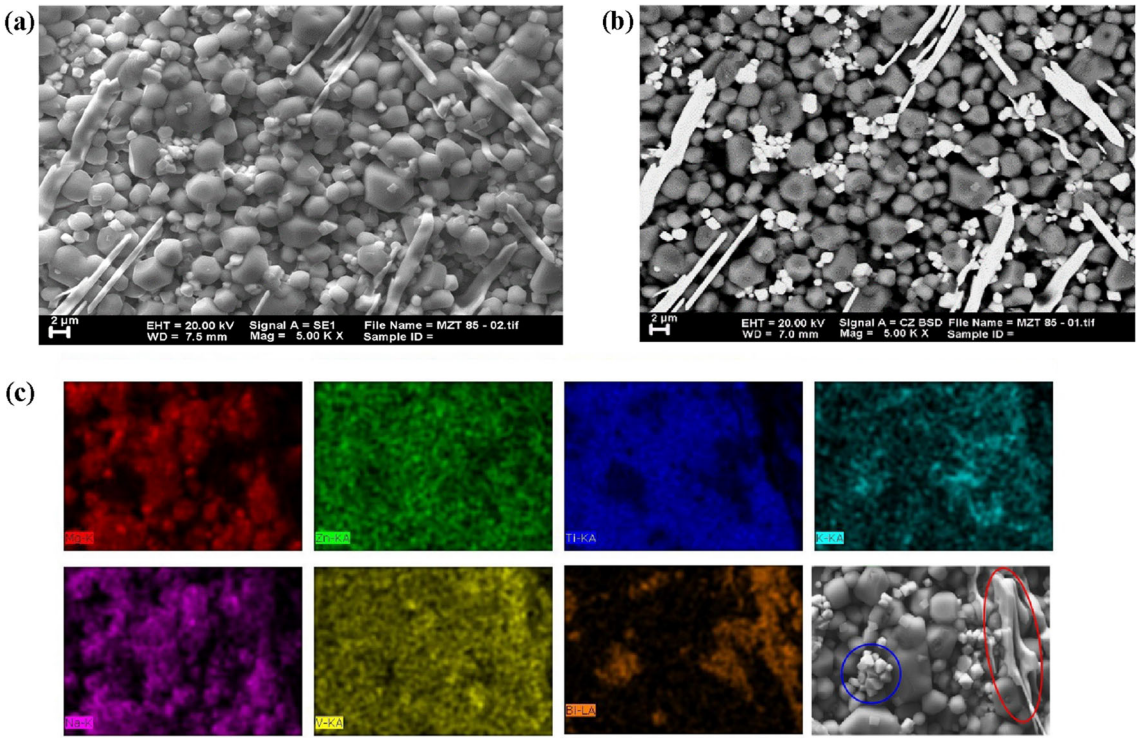


**Figure 3.** (**a**) SEM—secondary electron (SE) modes of thermally etched of MZT85 representative sample, (**b**) SEM—backscattered modes and (**c**) EDX micrograph of MZT85.

an elongated form supposed to be the precipitate of a liquid phase. After switching to backscattered mode, figure 3b, shows a bright contrast indicating that the small grain colonies and the precipitate phase contains heavier ions. Considering that the atomic number of Bi = 83, much higher than all atomic composers in the sample, bright images in backscattered mode are rich in Bi.

Further EDX analysis, figure 3c shows small size grains population rich in Bi, K (blue circled). This finding reinforces the XRD analysis earlier regarding the second phase present in the sample. Moreover, the elongated precipitate is rich in Bi and V and should be suspected as a precipitation of liquid phase comprising $Bi_2O_3$ and $V_2O_5$ amorphous (red circled).

### 3.2 *Dielectric properties*

The dielectric properties are shown in figure 4, indicating the relative permittivity, loss tangent and quality factor Qxf as a function of log frequency from 1 Hz up to $32 \times 10^6$ Hz and high frequency in the X-band zone $10^{9.9}$–$10^{10.1}$ Hz, respectively. The relative permittivity $\varepsilon_r$ should be distinguished into two zones, namely, space charges dipole polarization indicated by high loss tangent at low frequency characterized by an important decline of $\varepsilon_r$, then collapse when frequency increases, and the lattice dipole at high frequency characterized by almost constant $\varepsilon_r$ for various frequencies (figure 4a and b). The frequency at which transition occurs for all samples is depicted in table 2. The presence of sintering aids $Bi_2O_3$ and KNV (MZT85) provides $\varepsilon_r$ = 23.71, increase the sintering aids percentage, MZT75 and MZT65 the relative permittivity degrades to 15.54 and 18.40, respectively, besides the transition frequency is to increase at 0.8, 8 and 32 kHz. It should be compared to the undoped sample MZT, in which possesses a density ∼90% [7]. However, the transition frequency occurs at the lowest frequency (8 Hz), indicating that the MZT dominates by lattice dipole considering its almost pure phase, $\varepsilon_r$ = 15. The possible cause relates to the increase of the relative density for the advancement of relative permittivity for the doped sample. The shifted transition frequency is related to the dissolved dopant ions in the matrix creating defect and space charges, when $Bi^{3+}$ substitute $Mg^{2+}$ in A site ($Bi_{Mg}$) is compensated by a space charge $e'$ for neutralization, otherwise the secondary phase presence in these samples.

The X-band high-frequency permittivity characteristics of these samples show a 'sine' type curve ranging from 13 up to 20. These values are slightly smaller than dipole polarization described earlier, the discrepancy of $\varepsilon_r$ should arise from the different methods of measurement. Further, an increased dopant percentage on MZT75 and MZT65 samples, even though the transformation frequency of space

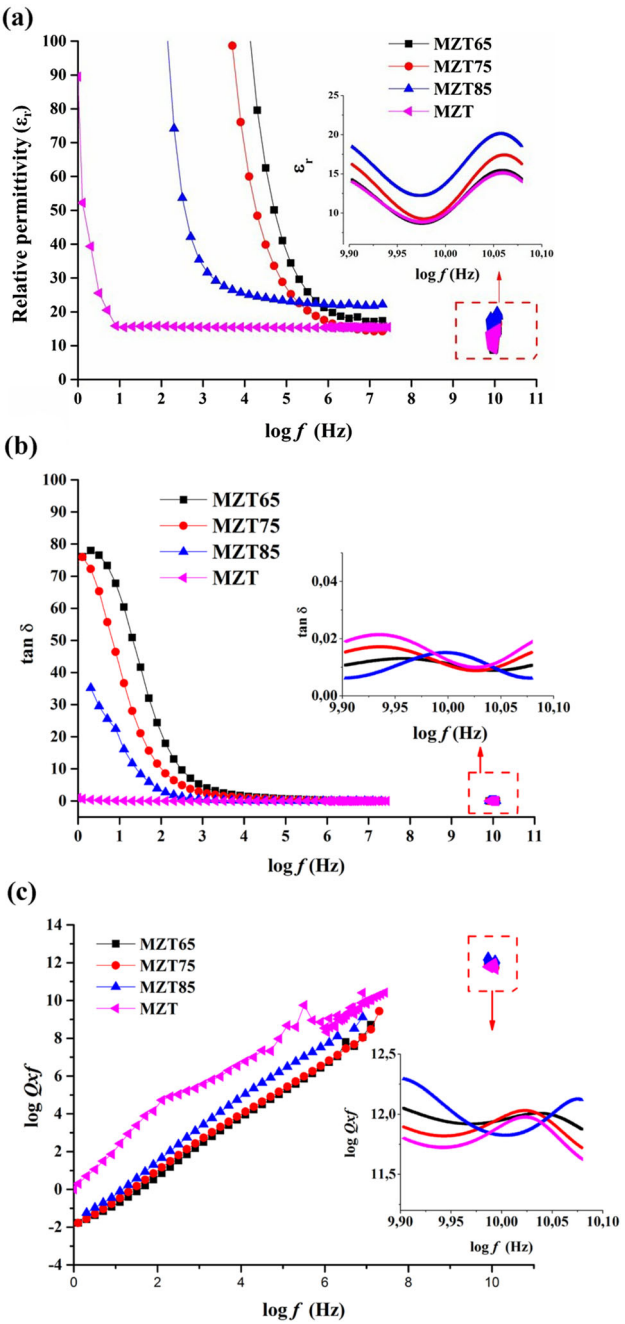


**Figure 4.** Dielectric properties of MZT–*x* samples characterized in this study as a function of log frequency. The MZT sample is used for comparison: (**a**) permittivity $\varepsilon_r$, (**b**) loss tangent and (**c**) log quality factor (Qxf).

charge and dipole polarization shifts to a higher frequency, those transitions are far below this range frequency, while the relative permittivity down to 15–18 close to the undoped sample 15. Furthermore, other characteristics loss tangent and Qxf have a similar trend. Considering the XRD analysis, these samples contain significant secondary phases; however, it is not degrading their characteristics at X-band frequency.

**Table 2.** Density, average permittivity at the dipole zone and the frequency at the transition zone.

| Sample | Relative density (%) | $<\varepsilon_r>$ at dipole zone (up to 32 MHz) | Transition frequency zone (kHz) | $<\varepsilon_r>$ at 10 GHz |
|---|---|---|---|---|
| MZT65 | 94.13 | 18.40 | 32 | 11.64 |
| MZT75 | 96.87 | 15.54 | 8 | 12.19 |
| MZT85 | 97.71 | 23.71 | 0.8 | 16.08 |
| MZT [7] | 90% | 15.10 | 0.008 | 13.50 |

## 4. Conclusion

The MZT-based ceramics material having composition $(0.95–x)Mg_{0.8}Zn_{0.2}TiO_3–xK_{0.5}Na_{0.5}VO_3–0.05Bi_2O_3$ ($x$ = 0.1–0.30) has been synthesized and characterized. By these compositions, the sintering temperature was completed as low as 950°C to attain relative density up to 97%. Analysis indicates that the KNV and $Bi_2O_3$ are partially dissolved in the MZT matrix creating defects, and the other parts perform secondary phases. These then intervene in the electrical properties at the 1 Hz–32 MHz domain, at low frequency is dominated by space charge outcome, the effect on permittivity then disappears at high frequency, and the remaining dipole polarization determines permittivity, the transition frequency of upturn with increasing $x$. The maximum permittivity value ($\varepsilon_r$) in the dipole polarization zone is given by the MZT85 sample with 16.08, the very low dielectric loss ($\tan\delta \sim 10^{-2}$). The dielectric properties of the samples with the KNV and $Bi_2O_3$ addition at high frequency (X-band) almost do not break the properties owned.

## References

[1] Chen X M, Li L and Liu X Q 2003 *Mater. Sci. Eng. B: Solid-State Mater. Adv.* **99** 255
[2] Looi M C 2007 Low sintering temperature of $MgTiO_3$ for type 1 capacitors. Jab. Kejuruter. Mek. Fak. Kejuruteraan, Univ. Malaya, Kuala Lumpur
[3] Huang C L and Chiang K H 2007 *J. Alloys Compd.* **431** 326
[4] Huang J B, Yang B, Yu C Y, Zhang G F, Xue H, Xiong Z X *et al* 2015 *Mater. Lett.* **138** 225
[5] Belnou F, Bernard J, Houivet D and Haussonne J M 2005 *J. Eur. Ceram. Soc.* **25** 2785
[6] Li L, Li S, Tian T, Lyu X, Ye J and Sun H 2016 *J. Mater. Sci. Mater. Electron.* **27** 1286
[7] Ermawati F U, Pratapa S, Suasmoro S, Hübert T and Banach U 2016 *J. Mater. Sci. Mater. Electron.* **27** 6637
[8] Tang B, Zhang S, Zhou X, Deng C and Yu S 2010 *J. Alloys Compd.* **492** 461
[9] Santhosh Kumar T and Pamu D 2015 *Mater. Sci. Eng. B Solid-State Mater. Adv. Technol.* **194** 86
[10] Ermawati F U, Suasmoro S and Pratapa S 2015 *Adv. Mater. Res.* **1112** 47

[11] Saukani M and Suasmoro S 2015 *Adv. Mater. Res.* **1112** 11
[12] Gogoi P, Singh L R and Pamu D 2017 *J. Mater. Sci. Mater. Electron.* **28** 11712
[13] Pan C L, Shen C H, Chen P C and Tan T C 2010 *J. Alloys Compd.* **503** 365
[14] Kathait G S, Panda M K and Panwar N S 2020 *Sci. Sinter.* **52** 97
[15] Chen C, Peng Z, Xie L, Bi K and Fu X 2020 *Int. J. Appl. Ceram. Technol.* **17** 2545
[16] Sebastian M T, Wang H and Jantunen H 2016 *Curr. Opin. Solid-State Mater. Sci.* **20** 151
[17] Liferovich R P and Mitchell R H 2005 *Phys. Chem. Miner.* **32** 442
[18] Chen Y Q, Li L, Ren Q, Zhu H T, Liang J K, Luo J *et al* 2011 *Chin. Phys. B* **20** 076402